molecular pharmaceutics

Article

pubs.acs.org/molecularpharmaceutics

^{99m}Tc-Labeled Cystine Knot Peptide Targeting Integrin $\alpha_v\beta_6$ for Tumor SPECT Imaging

Xiaohua Zhu,[†,‡] Jinbo Li,[†] Yeongjin Hong,[†,∥] Richard H. Kimura,[†] Xiaowei Ma,[†] Hongguang Liu,[†] Chunxia Qin,[†] Xiang Hu,[†] Thomas R. Hayes,[§] Paul Benny,[§] Sanjiv Sam Gambhir,[†] and Zhen Cheng*[,†]

[†]Molecular Imaging Program at Stanford (MIPS), Department of Radiology, and Bio-X Program, Canary Center at Stanford for Cancer Early Detection, Stanford University, Stanford, California 94305-5344, United States

[‡]Department of Nuclear Medicine, Tongji Hospital, Tongji Medical College, Huazhong University of Science and Technology, Wuhan, 430030, China

[§]Department of Chemistry, Washington State University, Pullman, Washington 99164, United States

[∥]Department of Microbiology, Chonnam National University Medical School, Gwangju 501-746, Republic of Korea

ABSTRACT: Integrin $\alpha_v\beta_6$ is overexpressed in a variety of cancers, and its expression is often associated with poor prognosis. Therefore, there is a need to develop affinity reagents for noninvasive imaging of integrin $\alpha_v\beta_6$ expression since it may provide early cancer diagnosis, more accurate prognosis, and better treatment planning. We recently engineered and validated highly stable cystine knot peptides that selectively bind integrin $\alpha_v\beta_6$ with no cross-reactivity to integrins $\alpha_v\beta_5$, $\alpha_5\beta_1$, or $\alpha_v\beta_3$, also known to be overexpressed in many cancers. Here, we developed a single photon emission computed tomography (SPECT) probe for imaging integrin $\alpha_v\beta_6$ positive tumors. Cystine knot peptide, $S_0$2, was first conjugated with a single amino acid chelate (SAAC) and labeled with $[^{99m}Tc(H_2O)_3(CO)_3]^+$. The resulting probe, ^{99m}Tc-SAAC-$S_0$2, was then evaluated by *in vitro* cell uptake studies using two $\alpha_v\beta_6$ positive cell lines (human lung adenocarcinoma cell line HCC4006 and pancreatic cancer cell line BxPC-3) and two $\alpha_v\beta_6$ negative cell lines (human lung adenocarcinoma cell line H838 and human embryonic kidney cell line 293T). Next, SPECT/CT and biodistribution studies were performed in nude mice bearing HCC4006 and H838 tumor xenografts to evaluate the *in vivo* performance of ^{99m}Tc-SAAC-$S_0$2. Significant differences in the uptake of ^{99m}Tc-SAAC-$S_0$2 were observed in $\alpha_v\beta_6$ positive vs negative cells ($P < 0.05$). Biodistribution and small animal SPECT/CT studies revealed that ^{99m}Tc-SAAC-$S_0$2 accumulated to moderate levels in antigen positive tumors (~2% ID/g at 1 and 6 h postinjection, $n = 3$ or 4/group). Moreover, the probe demonstrated tumor-to-background tissue ratios of 6.81 ± 2.32 (tumor-to-muscle) and 1.63 ± 0.18 (tumor-to-blood) at 6 h postinjection in $\alpha_v\beta_6$ positive tumor xenografts. Co-incubation of the probe with excess amount of unlabeled $S_0$2 as a blocking agent demonstrated significantly reduced tumor uptake, which is consistent with specific binding to the target. Renal filtration was the main route of clearance. In conclusion, knottin peptides are excellent scaffolds for which to develop highly stable imaging probes for a variety of oncological targets. ^{99m}Tc-SAAC-$S_0$2 demonstrates promise for use as a SPECT agent to image integrin $\alpha_v\beta_6$ expression in living systems.

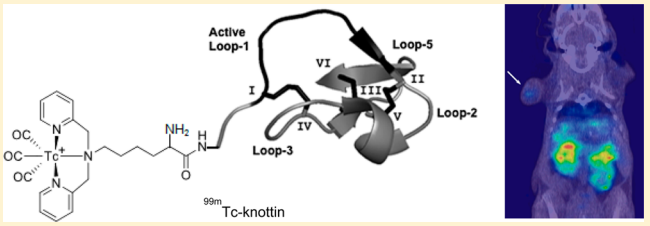

KEYWORDS: *integrin $\alpha_v\beta_6$, cystine-knot peptide, ^{99m}Tc, SPECT*

INTRODUCTION

Integrins are a large family of heterodimeric cell-surface glycoproteins that regulate cell adhesion, migration, proliferation, and apoptosis.[1] Changes in integrin expression and/or function are directly involved in tumor growth, angiogenesis, and metastasis, rendering these receptors promising diagnostic markers and potential therapeutic targets.[2−7] Integrin $\alpha_v\beta_6$ is up-regulated during morphogenesis, tumorigenesis, epithelial repair, and fibrosis of liver tissue.[8,9] The receptor is not constitutively expressed in normal tissues.[10,11] Recently, $\alpha_v\beta_6$ integrin has been shown to be a marker for epithelial-to-mesenchymal transition (EMT) crucial in the development of several types of tumors.[12] Indeed, $\alpha_v\beta_6$ integrin has been found to be expressed in pancreatic, gastric, lung, duodenal, colorectal, oral, and ovarian cancer, and its expression level is indicative of tumor aggressiveness.[13−21] In addition, $\alpha_v\beta_6$ integrin is a highly specific immunohistochemical marker for cholangiocarcinoma (CC), yielding specificity and a positive predictive value of 100% in differentiating CC from hepatocellular carcinoma (HCC).[22] Considering the aberrant expression of $\alpha_v\beta_6$ integrin in tumor biology, the development of noninvasive imaging techniques for integrin $\alpha_v\beta_6$ is needed for better cancer diagnosis, prognosis, and treatment planning.

Received: November 11, 2013
Revised: February 12, 2014
Accepted: February 13, 2014
Published: February 13, 2014

ACS Publications © 2014 American Chemical Society

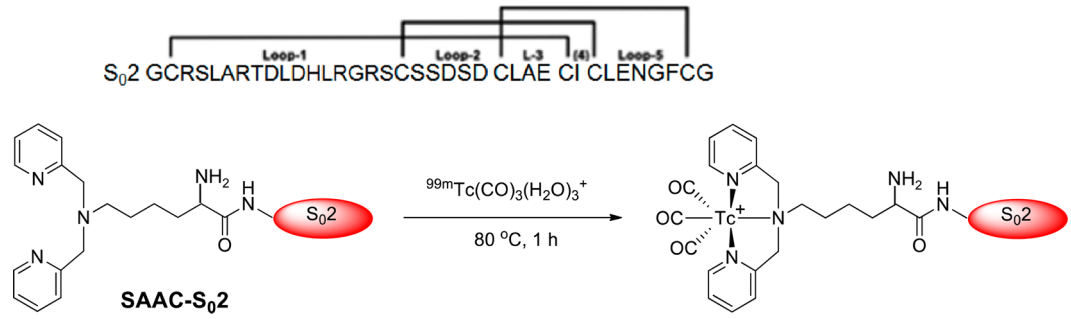

Figure 1. Synthetic scheme for ^{99m}Tc radiolabeling of SAAC-S02.

Several pioneering works have validated $\alpha_v\beta_6$ integrin as therapeutic and imaging targets.[23−29] The monoclonal antibody 10D5 has shown to successfully reduce the metastasis in lung cancers that overexpress $\alpha_v\beta_6$,[23] and a scFv, B63, has demonstrated the inhibition of $\alpha_v\beta_6$ mediated cell adhesion.[24] Linear or disulfide cyclized integrin $\alpha_v\beta_6$ binding peptides such as A20FMDV2 have been discovered and further used to develop positron emission tomography (PET) and single photon emission computed tomography (SPECT) probes.[25−28] More recently, cystine knot peptides (also known as knottins) have been developed as a novel class of $\alpha_v\beta_6$ binders.[29]

Knottins are small (3−4 kD) polypeptides with three interwoven disulfide bonds that define the central cysteine knot motif.[30] The cysteine knot motif may help these peptides withstand very harsh chemical, thermal, and proteolytic insults.[31] Knottin family members possess several surface-exposed loops that tolerate sequence diversity and are therefore amenable to directed evolution experiments.[32,33] In naturally occurring cystine knot peptides (knottins and cyclotides), these looped regions are responsible for a range of biological activities. Cystine knot peptides may be fitted with new bioactivities in these looped regions by rational design and library screening.[34−36] Since cystine knot peptides are relatively small, they demonstrate rapid and high tumor uptake as well as rapid clearance from nontargeted normal tissues.[37,38] Together, these characteristics make cystine knot peptides excellent candidates for diagnostic applications, particularly for tumor imaging, with high potential for clinical translation.

Using yeast surface display and protein engineering technologies, we recently identified and engineered several highly stable cysteine knot peptides, such as $S_0$2 and $R_0$1, that selectively bind integrin $\alpha_v\beta_6$ with single digit nanomolar binding affinities.[29] These new binders did not cross-react to related integrins such as $\alpha_v\beta_5$, $\alpha_5\beta_1$, or $\alpha_v\beta_3$. When conjugated with macrocyclic chelator 1,4,7,10-tetraazacyclododecane-1,4,7,10- tetraacetic acid (DOTA) at the N-terminus and labeled with PET radionuclide ^{64}Cu, both ^{64}Cu-DOTA-$S_0$2 and ^{64}Cu-DOTA-$R_0$1 demonstrated excellent PET images of integrin $\alpha_v\beta_6$ expressing pancreatic cancer in mice models.[29] ^{18}*F*-Fluorobenzoate labeled knottins ($S_0$2 and $R_0$1) also show translational promise for molecular imaging of integrin $\alpha_v\beta_6$ overexpression in pancreatic and other cancers.[39] Although PET has higher resolution and sensitivity, SPECT has several advantages over PET such as lower cost and more availability. ^{99m}Tc is the preferred radioisotope for SPECT applications because of its (1) favorable low-energy γ-emission (140 keV) and 6.02 h half-life, (2) availability from commercial ^{99}Mo-^{99m}Tc generators, and (3) low cost. It is considered the workhorse of nuclear medicine. Until now, neither the development of ^{99m}Tc-radiotracers for integrin $\alpha_v\beta_6$ imaging nor the use of ^{99m}Tc-labeled knottin probes has been reported. Therefore, in the present study, for the first time, a ^{99m}Tc labeled knottin SPECT tracer ($S_0$2) for integrin $\alpha_v\beta_6$ was prepared by conjugation of the knottin with a bifunctional chelate-single amino acid chelate (SAAC) and then labeled with ^{99m}Tc (Figure 1). Tumor uptake, biodistribution, and imaging of the resulting SPECT probe, ^{99m}Tc-SAAC-$S_0$2, were further evaluated in both integrin $\alpha_v\beta_6$-positive HCC4006 human lung adenocarcinoma and integrin $\alpha_v\beta_6$-negative H838 human lung adenocarcinoma xenograft mice models.

MATERIALS AND METHODS

Materials, Cell Lines, and Reagents. All 9-fluorenylmethyloxycarbonyl (Fmoc) protected amino acids were purchased from Novabiochem/EMD Chemicals Inc. (La Jolla, CA) with the exception of Fmoc-*N*-ε-1-(4,4-dimethyl-2,6-dioxocyclohex-1-ylidene)-3-methylbutyl-L-lysine [Fmoc-Lys (ivDde)-OH], which was purchased from Bachem (Torrance, CA), and Fmoc-L-Tyr(tBu)-Wang resin, which was purchased from CS Bio (Menlo Park, CA). Phosphate buffered saline (PBS) was from Gibco/Invitrogen (Carlsbad, CA). A single amino acid chelate (SAAC), Fmoc-Lys(DPA)-OH [(*S*)-2-((((9*H*-fluoren-9-yl)methoxy)carbonyl)amino)-6-(bis(pyridine-2-ylmethyl)-amino)hexanoic acid], was synthesized as previously described.[40] Isolink kits were obtained from Tyco, Inc. (Princeton, NJ). *N*,*N*′-Diisopropylethylamine (DIPEA) were purchased from Sigma-Aldrich Chemical Co. (St. Louis, MO). All other chemicals were purchased from Thermo Fisher Scientific (Pittsburgh, PA) unless otherwise specified. ^{99m}Tc-pertechnetate ($^{99m}TcO_4^-$) was purchased from Cardinal Health in Mountain View, CA and obtained from Stanford Nuclear Medicine Clinic. HCC4006 and H838 human lung adenocarcinoma cell lines and BxPC-3 pancreatic cancer cell line were obtained from American Type Culture Collection (Manassas, VA). Human embryonic kidney 293T cell line (HER293) was obtained from frozen laboratory stocks. Nude mice (nu/nu, female 4−5 weeks old) were purchased from Charles River Laboratory (Wilmington, MA).

Reversed-phase high performance liquid chromatography (RP-HPLC) was performed on a Dionex Summit HPLC system (Dionex Corporation, Sunnyvale, CA) equipped with a 170U 4-Channel UV−vis absorbance detector and radioactivity detector (Carroll & Ramsey Associates, model 105S, Berkeley, CA). UV detection wavelengths were set at 218, 254, and 280 nm for all the experiments. Both semipreparative (Vydac 218TP510-C18, 10 mm × 250 mm) and analytical (Dionex Acclaim120 C18, 4.6 mm × 250 mm) RP-HPLC columns were used. The mobile phase was solvent A [0.1% trifluoroacetic acid

dx.doi.org/10.1021/mp400683q | *Mol. Pharmaceutics* 2014, 11, 1208−1217

(TFA) in water] and solvent B [0.1% TFA in acetonitrile]. Matrix assisted laser desorption/ionization time-of-flight mass spectrometry (MALDI-TOF-MS) was performed on a Perceptive Voyager-DE RP Biospectrometry instrument (Framingham, MA) at the Stanford Protein and Nucleic Acid Biotechnology Facility (Stanford, CA).

Synthesis of SAAC-$S_0$2 Peptide Conjugate. An engineered cystine knot peptide $S_0$2 containing the sequence GCRSLARTDLDHLRGRCSSDSDCLAECICLENGFCG was synthesized on a CS336 sold-phase peptides synthesizer (CS Bio Co., Palo Alto, CA) using Fmoc-based solid phase peptide synthesis with Rink amide resin (CS Bio Co.) and folded as previously described.[29] For the conjugation reaction, SAAC (0.5 μmol) was activated with 0.5 μmol *O*-(*N*-succinimidyl)-*N*,*N*,*N*′,*N*′-tetramethyluronium tetrafluoroborate (TSTU) in 100 μL of dimethylformamide (DMF) containing 1% DIPEA at room temperature for 1 h. Knottin $S_0$2 (0.1 μmol) was reacted with the NHS ester of SAAC with gentle rocking overnight to yield SAAC-$S_0$2. The reaction mixture was analyzed and purified by RP-HPLC on a semipreparative C18 column. The flow rate was 3 mL/min, with the mobile phase starting from 95% solvent A and 5% solvent B (0−2 min) to 50% solvent A and 50% solvent B at 32 min. Fractions containing the product were collected (retention time 22.2 min) and lyophilized. The identity of SAAC-$S_0$2 was confirmed by MALDI-TOF-MS.

^{99m}Tc Radiolabeling. ^{99m}Tc labeling was accomplished in two steps using commercially available IsoLink kits. In the first step, $[^{99m}Tc(CO)_3(H_2O)_3]^+$ was prepared. Typically, $^{99m}TcO_4^-$ (740 MBq, 20 mCi) was added to an IsoLink kit, and the mixture was heated in an oil bath at 100 °C for 30 min. The solution was then cooled to 70 °Cand vented, and 1 N HCl was added to neutralize the solution to pH 5−6. In the second step, $[^{99m}Tc(CO)_3(H_2O)_3]^+$ in a sealed vial was mixed with 10 μg of SAAC-$S_0$2 (2.4 nmol) heated at 80 °C for 1 h. After the sample was cooled, the reaction mixture was analyzed by RP-HPLC. The ^{99m}Tc-complex, ^{99m}Tc-SAAC-$S_0$2, was then purified by RP-HPLC as described above with the mobile phase starting from 80% solvent A and 20% solvent B (0−2 min) to 60% solvent A and 40% solvent B at 32 min. The eluted fractions containing ^{99m}Tc-SAAC-$S_0$2 (retention time 22.6 min) were then collected, combined, and dried using a rotary evaporator. The radiochemical purity, defined as the ratio of the main product peak to other peaks, was determined by radio-HPLC to be >90%. The radiolabeled peptide was reconstituted in PBS (0.01 M, pH 7.4) and passed through a 0.22 μm Millipore filter into a sterile vial for cell culture and animal experiments.

***In Vitro* Stability.** *Serum Stability Assay.* ^{99m}Tc-SAAC-$S_0$2 (1.85 MBq, 50 μCi) was incubated in 500 μL of mouse serum (Sigma, St. Louis, MO) at 37 °C for 6 h. The mixture was filtered through a Microcon YM-10 10 kDa filter (EMD Millipore Corp, Billerica, MA). The samples were analyzed by radio-HPLC under identical conditions used to analyze the original radiolabeled compound. The percent of intact ^{99m}Tc-SAAC-$S_0$2 was determined by quantifying peaks corresponding to the intact and degraded products. The assays were repeated twice.

Amino Acid Challenge Assays. ^{99m}Tc-SAAC-$S_0$2 (1.85 MBq, 50 μCi) was incubated in 500 μL of solution containing L-cysteine at 1 mM in 10 mM PBS (pH 7.4) at 37 °C for 6 h. The sample was analyzed by radio-HPLC under conditions identical to those used to analyze the original radiolabeled compound. The percent of intact ^{99m}Tc-SAAC-$S_0$2 was determined by quantifying peaks corresponding to the intact product and to the degraded species. The assays were repeated twice.

Cell Culture and Tumor Xenograft Model. All of the human lung adenocarcinoma cell lines including HCC4006 ($\alpha_v\beta_6$-positive) and H838 ($\alpha_v\beta_6$-negative) and pancreatic cancer cell line BxPC-3 ($\alpha_v\beta_6$-positive[29]) were cultured in RPMI1640 media (Gibco, Carlsbad, CA) supplemented with 10% FBS and penicillin/streptomycin (all from Invitrogen, Grand Island, NY). The human embryonic kidney 293T cell line (HER293, $\alpha_v\beta_6$-negative[29]) was cultured in Dulbecco's modified Eagle's medium (DMEM, Gibco, Carlsbad, CA) with 10% fetal bovine serum (FBS) and penicillin/streptomycin. The cells were expanded in tissue culture dishes and kept in a humidified atmosphere of 5% CO_2 at 37 °C. The medium was changed every other day. A confluent monolayer was detached with 0.5% trypsin-EDTA in PBS (0.01 M, pH 7.4) and dissociated into a single-cell suspension for further cell culture and assays.

Animal procedures were carried out according to a protocol approved by the Stanford University Administrative Panels on Laboratory Animal Care (APLAC). Female athymic nude mice (nu/nu), obtained at 4−5 weeks of age, were injected subcutaneously in the left shoulder with 5×10^6 HCC4006 or H838 cells suspended in 100 μL of nonserum culture media with 50% (v/v) Matrigel. Mice were used for *in vivo* SPECT/computed tomography (CT) imaging and biodistribution studies when the tumors reached approximately 8 to 10 mm in diameter (4−6 weeks).

Study of $\alpha_v\beta_6$ Expression in Different Cell Lines. The copy number of integrin $\alpha_v\beta_6$ expressed on cells was quantitated by a fluorescence activated cell sorter (FACS) using antirat antibody coated Bangs standard beads (Bangs laboratories, IN) following the manufacturer's instructions. After discretizing cells with Trypsin-EDTA, cells (2.5×10^5) were stained with 1:100-diluted mouse antihuman integrin $\alpha_v\beta_6$ monoclonal antibody 10D5 (Millipore, Billerica, MA) in 100 μL of 0.1% BSA containing PBS (PBSA) for 30 min on ice. After washing, the cells were resuspended in 50 μL of PBSA, mixed with 50 μL of 1:50-diluted rat antimouse IgG-FITC (BioLegend, San Diego, CA) and incubated for 30 min on ice. At the same time, one drop (50 μL) of each Bangs beads was mixed with 50 μL of 1:50-diluted rat antimouse IgG-FITC and incubated for 30 min on ice. After washing, fluorescence mean values of each standard Bangs beads and cells were measured in FACS. The calibration plots of mean values of each Bangs standard beads against antibody binding concentration (ABC) were obtained in an Excel program provided by the manufacturer, and the number of integrin molecules on the cell surface was calculated using these plots.

***In Vitro* Cell Uptake Studies.** Cell uptake studies were performed as previously described.[41] Briefly, four cell lines (HCC4006, H838, BxPC-3, and 293T) were seeded at a density of 0.1×10^6 per well in 24-well tissue culture plates and were allowed to attach overnight. After gentle washing (3×) with serum-free culture medium, cells were incubated with ^{99m}Tc-SAAC-$S_0$2 (18.5 kBq, 0.5 μCi per well, in culture medium) with or without an excess amount of unlabeled integrin $\alpha_v\beta_6$-binding competitor, $S_0$2 (0.5 μg/well), at 37 °C for 0.5, 1, 2, 3, and 6 h. Cells incubated with $[^{99m}Tc(CO)_3(H_2O)_3]^+$ (same dose) were used as controls. Cells were then washed three times with chilled PBS containing 0.2% BSA and lysed with 0.5 M NaOH. Cell lysates were collected, and the radioactivity was measured using a gamma counter

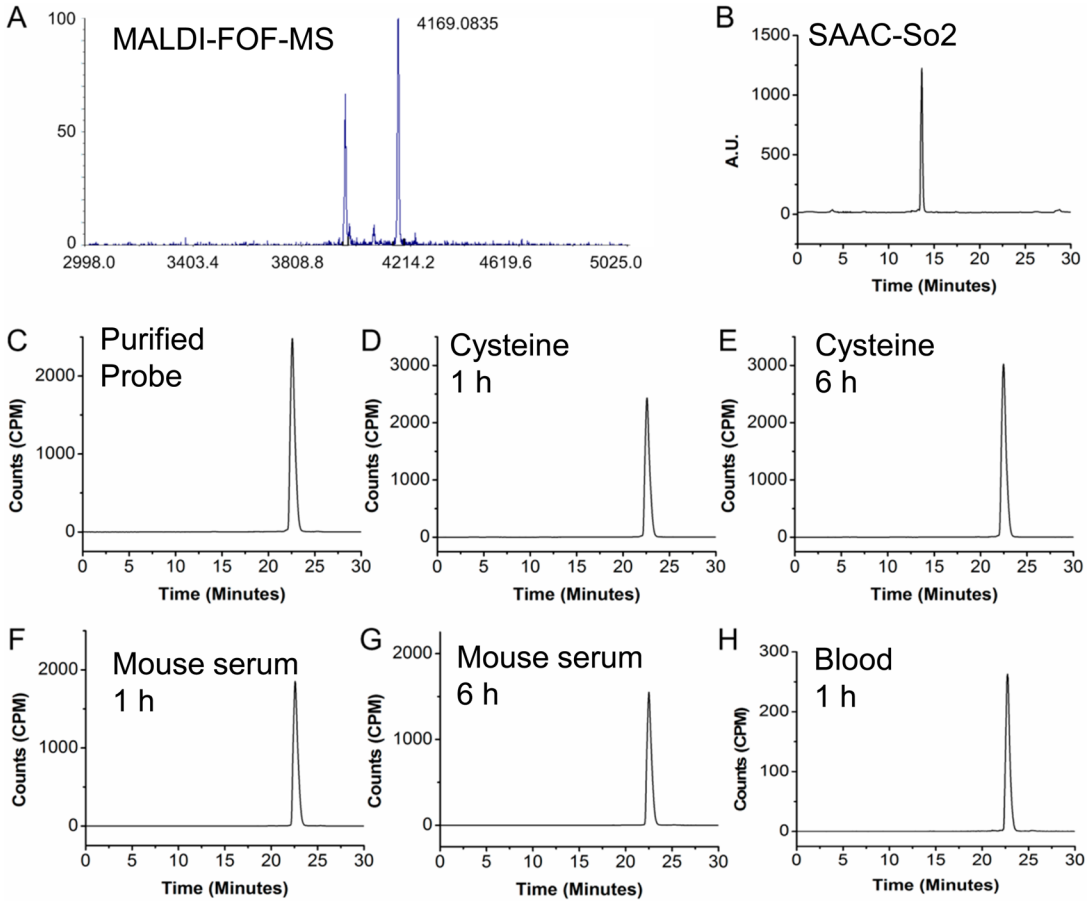

Figure 2. Characterization, stability, and *in vivo* metabolite analysis of ^{99m}Tc-SAAC-$S_0$2. MALDI-TOF-MS spectra of SAAC-$S_0$2 (A) and HPLC chromatogram of purified SAAC-$S_0$2 (B). HPLC radiochromatograms of purified ^{99m}Tc-SAAC-$S_0$2 in PBS (C) and the probe after incubation with cysteine (D and E) and mouse serum (F and G) at 37 °C for 1 and 6 h. Blood was analyzed by radio-HPLC at 1 h postinjection (H).

(PerkinElmer 1470, Waltham, MA). Cellular protein content was determined using a BCA protein assay kit. Cell uptake of ^{99m}Tc-SAAC-$S_0$2 was expressed as the percentage of added radioactive dose per milligram protein of cell (% AD/mg protein). Experiments were performed twice with quadruplicate wells.

Biodistribution Study and Metabolite Analysis. For biodistribution studies, anesthetized HCC4006 and H838 tumor-bearing mice (n = 4/group) were injected with ^{99m}Tc-SAAC-$S_0$2 (1.85 MBq, 50 μCi) via tail vein and sacrificed at 1 and 6 h after injection. Tumor and normal tissues of interest (blood, muscle, heart, liver, lungs, kidneys, spleen, brain, intestine, skin, stomach, and pancreas) were removed and wet weighed, and their radioactivity was measured with a gamma counter. The radioactivity uptake in the tumor and normal tissues was calculated and expressed as a percentage of the injected radioactive dose per gram of tissue (% ID/g). For each mouse, the activity of tissue samples was calibrated against a known aliquot of the radiotracer and normalized to the residual activity present in the tail.

A nude mouse was also injected with ^{99m}Tc-SAAC-$S_0$2 (7.4 MBq, 200 μCi) via the tail vein and was euthanized at 1 h p.i. Blood was centrifuged immediately after collection to remove the cells. The plasma portion was added with methanol (0.5 mL) with 1% Triton X-100. After centrifuging, the supernatant portion was diluted with solution A (99.9% H_2O with 0.1% TFA), and centrifuged again at 16,000g for 2 min with a nylon filter. The filtrate was analyzed by radio-HPLC under conditions identical to those used for analyzing the original radiolabeled peptide.

Small Animal SPECT/CT Imaging. Small animal SPECT/CT imaging was performed on a combined SPECT/CT scanner for small animals (X-SPECT; Gamma Medica, Salem, NH). Mice bearing HCC4006 and H838 xenografts (n = 3/group) were injected via the tail vein with approximately 7.4 MBq (200 μCi) of ^{99m}Tc-SAAC-$S_0$2. At 1 and 6 h postinjection (p.i.), mice were anesthetized with 2% isoflurane and placed in the prone position near the center of the field of view (FOV) of the scanner. For micro-CT image acquisition, 512 images (170 μm slice thickness) were acquired in 5 min at 0.4 mA and 80 kVp. SPECT was performed using a 1 mm multi pinhole collimator (single head, 360° rotation, 64 projections, 30 s/projection and a 5 cm FOV). CT images were reconstructed by using a cone-beam filtered back projection (FBP) algorithm into a 512 × 512 × 512 matrix with a voxel size of 170 μm. The SPECT images were reconstructed using a 2-dimensional ordered subsets expectation maximization (2D OSEM) algorithm with 8 subsets and 10 iterations into a 60 × 60 × 60 matrix size with a voxel size of 0.946 mm. All data were imported into Amira (Mercury Computing Systems, Chelmsford, MA) for processing and visualization.

Statistical Methods. All data were presented as the mean ± SD. Means were compared using Student's t test. A 95% confidence level was chosen to determine the significance

dx.doi.org/10.1021/mp400683q | *Mol. Pharmaceutics* 2014, 11, 1208−1217

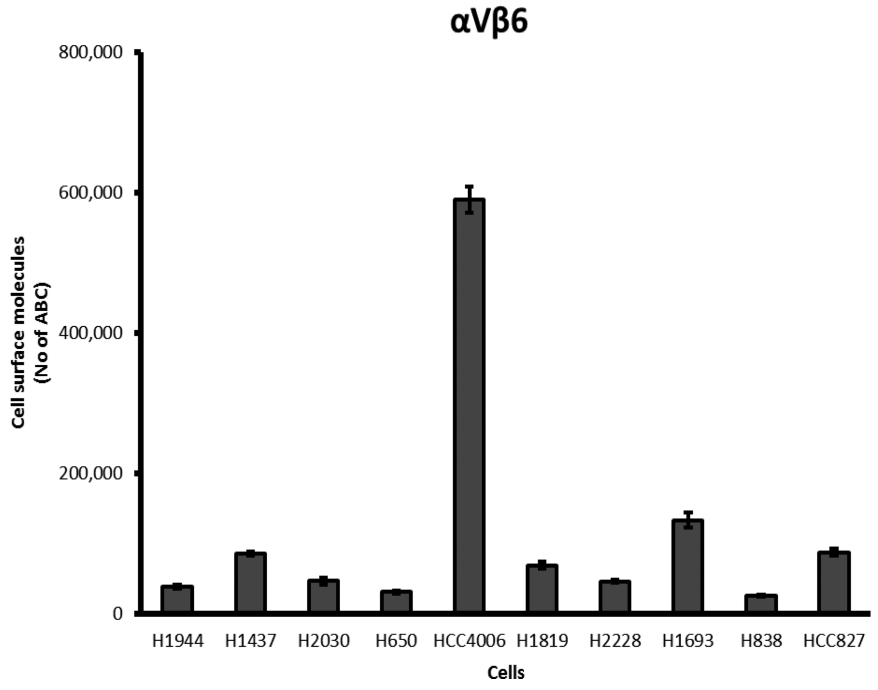

Figure 3. Integrin $\alpha_v\beta_6$ expression in different lung cancer cell lines.

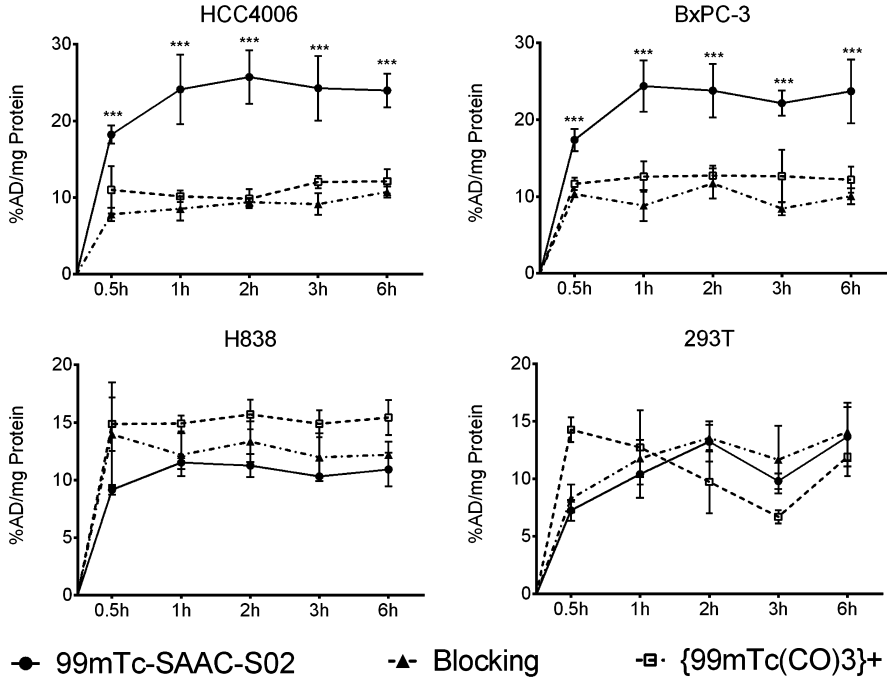

Figure 4. Four cell lines (HCC4006, H838, BxPC-3, and 293T) were incubated with ^{99m}Tc-SAAC-$S_0$2 (18.5 kBq, 0.5 μCi per well, in culture medium) with or without an excess amount of unlabeled integrin $\alpha_v\beta_6$-binding competitor, $S_0$2 (0.5 μg/well), at 37 °C for 0.5, 1, 2, 3, and 6 h. Cells incubated with $[^{99m}Tc(CO)_3(H_2O)_3]^+$ at the same dose were used as a control. Data are shown as the mean ± SD (n = 4). ***P < 0.05 for ^{99m}Tc-SAAC-$S_0$2 groups relative to blocking groups.

between groups, with P values of <0.05 indicating statistically significant differences.

RESULTS

Chemistry and Radiochemistry. Knottin $S_0$2 (MW 3871.3 Da) was synthesized, folded, and purified as described previously.[29] $S_0$2 was site specifically coupled with SAAC at the N-terminus with a yield of ∼25%. MALDI-TOF-MS analysis of the final products (purity of >95%, as determined by HPLC analysis) confirmed the absence of starting material and only the expected product. The measured MW (4169.1 Da) of the purified peptide was consistent with the expected MW (4166.7 Da) (Figure 2). SAAC-$S_0$2 was then radiolabeled with ^{99m}Tc with ∼40% radiochemical yield. After HPLC purification, the radiochemical purity of the resulting labeled peptide was over 90%. A modest specific activity of 14.8 MBq/nmol (0.4 Ci/

dx.doi.org/10.1021/mp400683q | Mol. Pharmaceutics 2014, 11, 1208−1217

Table 1. Biodistribution (Mean ± SD % ID/g) and the Tumor-to-Normal Tissue Ratios of ^{99m}Tc-SAAC-$S_0$2 in Lung Cancer Models (n = 4/Group)

	HCC4006		H838	
organs	1 h	6 h	1 h	6 h
tumor	2.02 ± 0.44[a]	2.09 ± 0.5$\hat{5}$	1.42 ± 0.14[a]	0.79 ± 0.0$\hat{7}$
blood	1.94 ± 0.23	1.29 ± 0.32	2.61 ± 0.23	1.19 ± 0.25
heart	1.26 ± 0.11	0.56 ± 0.09	1.30 ± 0.12	0.54 ± 0.34
lungs	2.15 ± 0.26	2.00 ± 0.49	2.89 ± 0.44	1.80 ± 0.71
liver	4.19 ± 0.47	2.04 ± 0.23	4.02 ± 0.83	2.19 ± 0.41
spleen	1.31 ± 0.21	0.63 ± 0.06	1.29 ± 0.24	0.75 ± 0.18
pancreas	0.78 ± 0.14	0.53 ± 0.08	0.69 ± 0.26	0.54 ± 0.12
stomach	13.03 ± 2.49	8.69 ± 2.44	14.63 ± 1.18	7.97 ± 2.40
brain	0.09 ± 0.03	0.05 ± 0.01	0.09 ± 0.04	0.06 ± 0.02
intestine	1.65 ± 0.36	0.66 ± 0.12	1.57 ± 0.47	0.64 ± 0.04
kidneys	29.71 ± 3.56	17.89 ± 2.48	27.46 ± 4.09	17.88 ± 4.65
skin	0.93 ± 0.18	0.65 ± 0.17	0.61 ± 0.04	0.62 ± 0.10
muscle	0.44 ± 0.12	0.35 ± 0.19	0.65 ± 0.11	0.34 ± 0.03
bone	0.54 ± 0.13	0.44 ± 0.15	0.64 ± 0.14	0.38 ± 0.07
ratios				
tumor/muscle	4.77 ± 1.36	6.81 ± 2.32	2.26 ± 0.54	2.32 ± 0.13
tumor/blood	1.04 ± 0.15	1.63 ± 0.18	0.55 ± 0.71	0.69 ± 0.14
tumor/liver	0.48 ± 0.06	1.02 ± 0.20	0.36 ± 0.07	0.37 ± 0.07
tumor/kidneys	0.07 ± 0.02	0.12 ± 0.34	0.05 ± 0.01	0.05 ± 0.01
tumor/lung	0.94 ± 0.15	1.06 ± 0.17	0.52 ± 0.11	0.49 ± 0.18

[a] t = 0.037, P < 0.05; $\hat{t}$ = 0.073, P < 0.05.

μmol) of ^{99m}Tc-SAAC-$S_0$2 was obtained at the end of synthesis (decay-corrected).

***In Vitro* and *In Vivo* Stability.** The stability of radiotracers in physiological media is essential for optimal nuclear imaging. Therefore, the *in vitro* stability of ^{99m}Tc-SAAC-$S_0$2 was assessed for 6 h at 37 °C in mouse serum or in cysteine solutions (transchelation) at pH 7.4, and the results are shown in Figure 2. More than 90% of the radiolabeled complex remained unaltered after 6 h of incubation in mouse serum or in the 1 mM cysteine solution. Moreover, the probe was highly stable in blood and was intact at 1 h postinjection (Figure 2). ^{99m}Tc-SAAC-$S_0$2 resisted degradation or transchelation, which warrants its further exploration for targeting $\alpha_v\beta_6$ *in vitro* and *in vivo*.

$\alpha_v\beta_6$ Expression in Cell Lines Tested. Ten different lung cancer cell lines were evaluated for integrin $\alpha_v\beta_6$ expression on the cell surface using Bangs calibration standard beads as described above and in the manufacturer's instructions. Nine of the 10 cell lines tested low in integrin $\alpha_v\beta_6$ (≤100,000 copies per cell), and H838 cells were the lowest (26,000 copies per cell). However, one cell line, HCC4006, exhibited much higher integrin $\alpha_v\beta_6$ expression (>600,000 copies per cell) (Figure 3). In unpublished proteomics studies, this same cell line demonstrated more EMT markers than the other cell lines tested here. Since we were looking for integrin $\alpha_v\beta_6$-high and -low cell lines, we chose HCC4006 and H838, respectively, to fulfill these requirements for *in vivo* validation of the cancer marker and the SPECT tracer under development.

Cell Uptake of ^{99m}Tc-SAAC-$S_0$2. Cell uptake assays of ^{99m}Tc-SAAC-$S_0$2 were performed to evaluate specific $\alpha_v\beta_6$ targeting. Four cell lines were used. HCC4006 and BxPC-3 both express high levels of integrin $\alpha_v\beta_6$, whereas H838 and 293T express low and no integrin $\alpha_v\beta_6$, respectively. Cells were incubated with ^{99m}Tc-SAAC-$S_0$2 for 0.5 h, 1 h, 2 h, 3 h, and 6 h at 37 °C, compared with the control group incubated with $[^{99m}Tc(CO)_3]^+$. There were significant differences in cell uptake over time between $\alpha_v\beta_6$ positive cells and $\alpha_v\beta_6$ negative cells (P < 0.05) (Figure 4). High accumulation was found in both HCC4006 and BxPC-3 cells, reaching 18.2 ± 0.3 and 17.4 ± 1.4%AD/mg protein, respectively. As expected, low accumulation similar to that of the control groups (cell uptake of $[^{99m}Tc(CO)_3]^+$) was found in both H838 and 293T cells; 9.2 ± 0.4 and 7.3 ± 0.9%AD/mg protein, respectively, were observed after 0.5 h of incubation. Uptake in HCC4006 and BXPC-3 cells increased to 24.1 ± 4.5 and 24.4 ± 3.3%AD/mg protein, respectively, at 1 h and maintained the same level until the 6 h time point.

To further confirm whether the binding of ^{99m}Tc-SAAC-$S_0$2 with cells was specific for $\alpha_v\beta_6$, the cells were incubated with solutions containing both ^{99m}Tc-SAAC-$S_0$2 and excess amounts of unlabeled $S_0$2 as the blocking agent. As shown in Figure 4, uptake in both $\alpha_v\beta_6$ positive HCC4006 and BxPC-3 cells markedly reduced to less than 50% that of being incubated with ^{99m}Tc-SAAC-$S_0$2 alone (P < 0.05), similar to those of the control group. However, there was no decreased uptake (P > 0.05) observed in H838 or 293T cells ($\alpha_v\beta_6$ negative). Thus, the unlabeled $S_0$2 significantly blocked the binding of ^{99m}Tc-SAAC-$S_0$2 to $\alpha_v\beta_6$ positive cells, indicating that the probe specifically targets integrin $\alpha_v\beta_6$.

Biodistribution Studies with ^{99m}Tc-SAAC-$S_0$2. The *in vivo* biodistribution of ^{99m}Tc-SAAC-$S_0$2 in mice bearing HCC4006 or H838 lung cancers was determined at 1 and 6 h time points after intravenous injection of the probe (Table 1). The normal tissue uptake in mice bearing the HCC4006 or H838 tumor was similar and decreased with time, but the tumor uptake of the HCC4006 xenograft was significantly higher than that of the H838 xenograft, being 2.02 ± 0.44% ID/g and 2.09 ± 0.55% ID/g vs 1.42 ± 0.14% ID/g and 0.79 ± 0.07% ID/g (P < 0.05) at 1 and 6 h after injection, respectively. ^{99m}Tc-SAAC-$S_0$2 demonstrated better retention in $\alpha_v\beta_6$ positive tumors compared to that in $\alpha_v\beta_6$ negative tumors and normal tissue. Higher probe uptake was observed in the kidneys in all

dx.doi.org/10.1021/mp400683q | *Mol. Pharmaceutics* 2014, 11, 1208−1217

mice with a value of 29.7 ± 3.6% ID/g and 17.8 ± 2.5% ID/g in HCC4006 xenograft mice or 27.5 ± 4.1% ID/g and 17.9 ± 4.7% ID/g in H838 xenograft mice at 1 and 6 h, respectively. Accumulation of the probe in the liver was relatively low, with a value of 4.19 ± 0.47% ID/g and 2.04 ± 0.23% ID/g in HCC4006 xenograft mice or 4.02 ± 0.83% ID/g and 2.19 ± 0.41% ID/g in H838 xenograft mice at 1 and 6 h, respectively. These data indicate that the probe is mainly excreted and metabolized by the kidneys. Moreover, ^{99m}Tc-SAAC-$S_0$2 displayed very low muscle uptake of 0.44 ± 0.12% ID/g and 0.65 ± 0.11% ID/g at 1 h after injection in HCC4006 and H838 xenograft mice, respectively, which decreased to 0.35 ± 0.19% ID/g and 0.34 ± 0.03% ID/g at 6 h after injection. However, the blood clearance of ^{99m}Tc-SAAC-$S_0$2 was somewhat slow, being 1.94 ± 0.23% ID/g and 1.29 ± 0.32% ID/g in HCC4006 xenograft mice or 2.61 ± 0.23% ID/g and 1.19 ± 0.25% ID/g in H838 xenograft mice at 1 and 6 h, respectively.

Tumor-to-background tissue ratios in HCC4006 xenograft mice were higher than those in H838 xenograft mice ($P < 0.05$, $n = 4$/group). The ratios increased over time for HCC4006 tumor mice but not in H838 xenograft mice (Table 1), suggesting the specific targeting of the probe as well. For example, tumor-to-blood and tumor-to-muscle ratios increased from 1.04 ± 0.15 and 4.77 ± 1.36 at 1 h postinjection to 1.63 ± 0.18 and 6.81 ± 2.32 at 6 h postinjection in HCC4006 xenograft mice, which bodes well for the application of ^{99m}Tc-SAAC-$S_0$2 as an *in vivo* molecular imaging agent.

Small Animal SPECT/CT. Representative coronal small animal SPECT/CT images of HCC4006 xenograft mice and H838 xenograft mice ($n = 3$/group) at 1 h after injection are shown in Figure 5. Only the HCC4006 xenograft was visible, and moderate tumor-to-background contrast was achieved, suggesting that ^{99m}Tc-SAAC-$S_0$2 might be useful for imaging the $\alpha_v\beta_6$ positive tumor. High accumulation of radioactivity was observed in the kidneys, which confirmed that the probe was excreted by the kidneys.

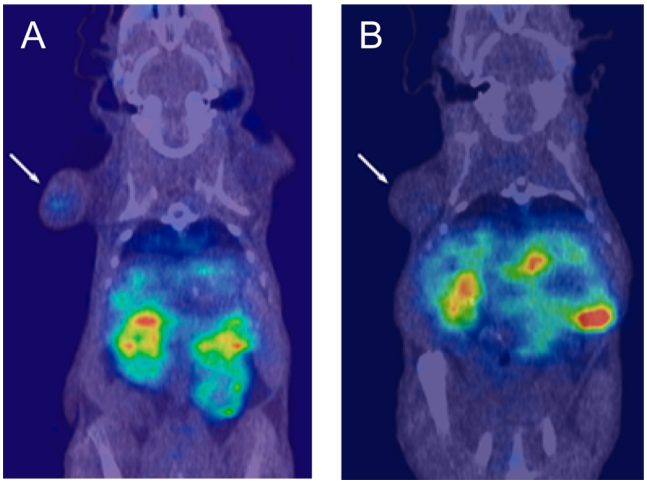

Figure 5. Coronal SPECT/CT images of a mouse bearing HCC4006 xenograft (A) and a mouse bearing H838 xenograft (B) at 1 h postinjection of 7.4 MBq of ^{99m}Tc-SAAC-$S_0$2.

DISCUSSION

Novel nonimmunogenic scaffold based peptides have increasingly become the focus of attention for molecular probe design and development because of their stable structure, easy synthesis, low cost, site specific labeling, and high affinity targeting to many different cancer markers.[38] Among these, engineered knottins have shown promise in molecular imaging applications. In our previous studies, RGD-containing cysteine knot peptides, based on the EETI-II or AgRP scaffolds, have been used as affinity reagents to deliver contrast agents to tumors in order to evaluate several different imaging modalities.[37,42−50] Recently, a new set of cysteine knot peptides based on MCoTI-II and LCTI-I has been engineered to bind integrin $\alpha_v\beta_6$ with single digit nanomolar affinities. Biocombinatorial cystine knot libraries displayed on the surface of yeast display were sorted by FACS to generate several bioactive loops that bind integrin $\alpha_v\beta_6$. One particular activity, "2" (RSLAR-TDLDHLRGR), was engrafted into several different cystine knot scaffolds with biased amino acid content (R_0, E_0 and S_0).[29] The preliminary small animal PET imaging results showed that $S_0$2 and $R_0$1 were promising candidates for further explorations.[29,39] Here, for the first of time, we report the ^{99m}Tc labeled knottin $S_0$2, ^{99m}Tc-SAAC-$S_0$2, as a novel SPECT probe for integrin $\alpha_v\beta_6$ positive tumor imaging. Compared to some other developed integrin $\alpha v\beta 6$ targeted PET radiotracers, the ^{99m}Tc-probe is cheaper and can be available worldwide. Moreover, it can be easily prepared even in kit form. The easy labeling chemistry and low energy of ^{99m}Tc can also reduce the radiation dose to radiochemists and patients.

SAAC is a novel bifunctional chelate constructed from derivatized amino acids modified to provide three donor groups (L3) for chelation to the $[^{99m}Tc(CO)_3]^+$ core. SAAC derivatives demonstrate facile labeling with ^{99m}Tc. ^{99m}Tc-SAAC-$S_0$2 demonstrates robust stability toward cysteine and histidine challenge, which effectively compete *in vivo* for these ligands.[51] SAAC avoids many problems associated with using sulfhydryl-containing radioligands and chelating agents that do not fully occupy the coordination sites of ^{99m}Tc, which results in the formation of unstable complexes. In addition, SAAC may be incorporated into bioactive peptides via standard solid phase peptide synthesis and subsequently labeled with ^{99m}Tc and $^{186/188}$Re.[52] In this work, we chose to couple SAAC onto the $S_0$2 peptide in solution via robust TSTU/DIPEA activation and amidation reactions. ^{99m}Tc labeling is straightforward with decent radiochemical purity, yield, and reasonable specific activity, suitable for *in vivo* testing. Furthermore, the *in vitro* and *in vivo* stability assays demonstrate that ^{99m}Tc-SAAC-$S_0$2 is highly stable under different conditions (mouse serum and cysteine challenge, Figure 2), which is consistent with the high stability of knottins reported before.[31]

The *in vitro* cell uptake studies show significant differences between $\alpha_v\beta_6$ positive cells and $\alpha_v\beta_6$ negative cells (Figure 3). Uptake values in integrin $\alpha_v\beta_6$ positive cells are also effectively blocked by an excess of unlabeled $S_0$2, further confirming the target-binding specificity of ^{99m}Tc-SAAC-$S_0$2. The pattern of ^{99m}Tc-SAAC-$S_0$2 in the cell uptake study is consistent with the *in vivo* studies of xenograft models. ^{99m}Tc-SAAC-$S_0$2 uptake in integrin $\alpha_v\beta_6$ positive cells reaches a plateau at the 1 h time point and remains almost unaltered to the 6 h time point in integrin positive cells. However, ^{99m}Tc-SAAC-$S_0$2 uptake in integrin negative cells show significantly lower uptake over the same time. Biodistribution studies revealed persistent radiotracer uptake in integrin $\alpha_v\beta_6$ positive tumors. Some nonspecific uptake was observed in integrin $\alpha_v\beta_6$ negative tumors at early time points, but this background effectively cleared over time.

Furthermore, moderate tumor/muscle ratios in integrin positive HCC4006 xenograft mice are observed and increased from 4.77 ± 1.36 at 1 h postinjection to 6.81 ± 2.32 at 6 h postinjection, indicating good contrast for tumor imaging. The tumor/muscle ratios in H838 xenograft mice are rather low, which is consistent with the lack of integrin $\alpha_v\beta_6$ expression in these tumor models. High accumulation of radioactivity was also observed in the kidneys by SPECT at both the 1 and 6 h time points, which confirmed a renal clearance route. Biodistribution studies were in agreement with SPECT studies where good tumor contrast was achieved as early as 1 h post injection. Off target accumulation in the kidney, liver, and gut were also in agreement with SPECT studies. Lastly, the specific cell uptake and tumor targeting ability of ^{99m}Tc-SAAC-$S_0$2 as verified by cell and animal studies also indicates that SAAC-$S_0$2 can endure the labeling and purification conditions and preserve its bioactivity.

Compared to the previously reported PET probe ^{64}Cu-DOTA-$S_0$2,[29] ^{99m}Tc-SAAC-$S_0$2 demonstrated several positive features such as quick tumor targeting and rapid renal clearance. For example, ^{99m}Tc-SAAC-$S_0$2 displays kidney uptake similar to that of ^{64}Cu-DOTA-$S_0$2 (29.71 ± 3.56% ID/g vs 26.53 ± 12.26% ID/g, respectively, at 1 h), suggesting that for the ^{99m}Tc-SAAC labeled cystine knot, the reduction in off target radiation exposure bodes well for translation. For other tissues, ^{64}Cu-DOTA-$S_0$2 exhibits low uptake in blood and liver (0.46 ± 0.18% ID/g and 2.28 ± 0.40% ID/g, respectively, at 1 h) and high tumor/blood and tumor/liver ratio, whereas the blood and liver uptake of ^{99m}Tc-SAAC-$S_0$2 is quite high (1.94 ± 0.23% ID/g and 4.19 ± 0.47% ID/g, respectively at 1 h), and its tumor/blood and tumor/liver ratios are quite low. The high blood and liver uptake and retention observed is likely attributed to the high lipophilicity associated with the ^{99m}Tc-$(CO)_3$ core, which could slow down the clearance rate of the tracer. This general trend with ^{99m}Tc$(CO)_3$ appended systems has been observed with other peptides.[53,54] Moreover, high stomach uptake was also observed, which may be caused by ^{99m}Tc$(CO)_3$ labeling. The high lipophilicty of the ^{99m}Tc$(CO)_3$ label could also increase the nonspecific uptake of the probe in the tumor, resulting in a small difference in the uptake between two tumor models (Table 1). These data highlight the necessity of further improving the *in vivo* performance of ^{99m}Tc labeled cystine knot peptides. Chelators that are less hydrophobic in addition to different ^{99m}Tc labeling methods [for example,^{99m}TcO(V)] could be explored to develop SPECT probes with better *in vivo* performance.

CONCLUSION

In this study, we successfully developed a cystine knot SPECT probe (^{99m}Tc-SAAC-$S_0$2) which allows the imaging of integrin $\alpha_v\beta_6$ positive tumors. The probe demonstrates integrin $\alpha_v\beta_6$ target-binding specificity *in vitro* and *in vivo*, and can clearly identify integrin $\alpha_v\beta_6$ positive tumors in living animals. The initial results for ^{99m}Tc-SAAC-$S_0$2 are promising so that further development and evaluation as a SPECT agent are warranted for a low-cost integrin $\alpha_v\beta_6$ imaging option. The cystine knot scaffold appears to be an excellent platform from which to develop SPECT and PET imaging probes for a variety of targets such as integrin family members.

AUTHOR INFORMATION

Corresponding Author

*Molecular Imaging Program at Stanford, Department of Radiology and Bio-X Program, Canary Center at Stanford for Cancer Early Detection, 1201 Welch Road, Lucas Expansion, P095 Stanford University, Stanford, CA 94305-5484. Phone: 650-723-7866. Fax: 650-736-7925. E-mail: zcheng@stanford.edu.

Notes

The authors declare no competing financial interest.

ACKNOWLEDGMENTS

This work was supported, in part, by the Office of Science (BER), U.S. Department of Energy (DE-SC0008397), NCI In Vivo Cellular Molecular Imaging Center (ICMIC) grant P50 CA114747, and the National Natural Science Foundation of China (No. 86271600). We thank Ayumu Taguchi, Samir Hanash, and Adi Gazdar for providing the cell lines used in this study.

ABBREVIATIONS

SPECT, single photon emission computed tomography; HPLC, high-performance liquid chromatography; SAAC, single amino acid chelate; % ID/g, % injected radioactive dose per gram of tissue; % AD/mg protein, % added radioactive dose per milligram of protein; p.i., postinjection; FACS, fluorescence-activated cell sorter

REFERENCES

(1) Hynes, R. O. Integrins: bidirectional, allosteric signaling machines. *Cell* **2002**, *110* (6), 673−687.

(2) Volpes, R.; van den Oord, J. J.; Desmet, V. J. Integrins as differential cell lineage markers of primary liver tumors. *Am. J. Pathol.* **1993**, *142* (5), 1483−1492.

(3) Mizejewski, G. J. Role of integrins in cancer: survey of expression patterns. *Proc. Soc. Exp. Biol. Med.* **1999**, *222* (2), 124−138.

(4) Van Waes, C. Cell adhesion and regulatory molecules involved in tumor formation, hemostasis, and wound healing. *Head Neck* **1995**, *17* (2), 140−147.

(5) Eble, J. A.; Haier, J. Integrins in cancer treatment. *Curr. Cancer Drug Targets* **2006**, *6* (2), 89−105.

(6) Pignatelli, M.; Cardillo, M. R.; Hanby, A.; Stamp, G. W. Integrins and their accessory adhesion molecules in mammary carcinomas: loss of polarization in poorly differentiated tumors. *Hum. Pathol.* **1992**, *23* (10), 1159−1166.

(7) Bandyopadhyay, A.; Raghavan, S. Defining the role of integrin alphavbeta6 in cancer. *Curr. Drug Targets* **2009**, *10* (7), 645−652.

(8) Patsenker, E.; Popov, Y.; Stickel, F.; Jonczyk, A.; Goodman, S. L.; Schuppan, D. Inhibition of integrin alphavbeta6 on cholangiocytes blocks transforming growth factorbeta activation and retards biliary fibrosis progression. *Gastroenterology* **2008**, *135* (2), 660−670.

(9) Popov, Y.; Patsenker, E.; Stickel, F.; Zaks, J.; Bhaskar, K. R.; Niedobitek, G.; Kolb, A.; Friess, H.; Schuppan, D. Integrin alphavbeta6 is a marker of the progression of biliary and portal liver fibrosis and a novel target for antifibrotic therapies. *J. Hepatol.* **2008**, *48* (3), 453−464.

(10) Breuss, J. M.; Gallo, J.; DeLisser, H. M.; Klimanskaya, I. V.; Folkesson, H. G.; Pittet, J. F.; Nishimura, S. L.; Aldape, K.; Landers, D. V.; Carpenter, W.; Gillett, N.; Sheppard, D.; Matthay, M. A.; Albelda, S. M.; Kramer, R. H.; Pytela, R. Expression of the beta 6 integrin subunit in development, neoplasia and tissue repair suggests a role in epithelial remodeling. *J. Cell Sci.* **1995**, *108* (6), 2241−2251.

(11) Breuss, J. M.; Gillett, N.; Lu, L.; Sheppard, D.; Pytela, R. Restricted distribution of integrin beta 6 mRNA in primate epithelial tissues. *J. Histochem. Cytochem.* **1993**, *41* (10), 1521−1527.

(12) Lee, J. M.; Dedhar, S.; Kalluri, R.; Thompson, E. W. The epithelial-mesenchymal transition: new insights in signaling, development, and disease. *J. Cell Biol.* **2006**, *172* (7), 973−981.
(13) Sipos, B.; Hahn, D.; Carceller, A.; Piulats, J.; Hedderich, J.; Kalthoff, H.; Doodman, S. L.; Kosmahl, M.; Kloppel, G. Immunohistochemical screening for beta6-integrin subunit expression in adenocarcinomas using a novel monoclonal antibody reveals strong upregulation in pancreatic ductal adenocarcinomas in vivo and in vitro. *Histopathology* **2004**, *45* (3), 226−236.
(14) Xue, H.; Atakilit, A.; Zhu, W.; Li, X.; Ramos, D. M.; Pytela, R. Role of the alpha(v)beta6 integrin in human oral squamous cell carcinoma growth in vivo and in vitro. *Biochem. Biophys. Res. Commun.* **2001**, *288* (3), 610−618.
(15) Regezi, J. A.; Ramos, D. M.; Pytela, R.; Dekker, N. P.; Jordan, R. C. Tenascin and beta 6 integrin are overexpressed in floor of mouth in situ carcinomas and invasive squamous cell carcinomas. *Oral Oncol.* **2002**, *38* (4), 332−336.
(16) Ahmed, N.; Riley, C.; Rice, G. E.; Quinn, M. A.; Baker, M. S. Alpha(v)beta(6) integrin-A marker for the malignant potential of epithelial ovarian cancer. *J. Histochem. Cytochem.* **2002**, *50* (10), 1371−1380.
(17) Ahmed, N.; Pansino, F.; Clyde, R.; Murthi, P.; Quinn, M. A.; Rice, G. E.; Agrez, M. V.; Mok, S.; Baker, M. S. Overexpression of alpha(v)beta6 integrin in serous epithelial ovarian cancer regulates extracellular matrix degradation via the plasminogen activation cascade. *Carcinogenesis* **2002**, *23* (2), 237−244.
(18) Kawashima, A.; Tsugawa, S.; Boku, A.; Kobayashi, M.; Minamoto, T.; Nakanishi, I.; Oda, Y. Expression of alphav integrin family in gastric carcinomas: increased alphavbeta6 is associated with lymph node metastasis. *Pathol. Res. Pract.* **2003**, *199* (2), 57−64.
(19) Hazelbag, S.; Kenter, G. G.; Gorter, A.; Dreef, E. J.; Koopman, L. A.; Violette, S. M.; Weinreb, P. H.; Fleuren, G. J. Overexpression of the alpha v beta 6 integrin in cervical squamous cell carcinoma is a prognostic factor for decreased survival. *J. Pathol.* **2007**, *212* (3), 316−324.
(20) Bates, R. C.; Bellovin, D. I.; Brown, C.; Maynard, E.; Wu, B.; Kawakatsu, H.; Sheppard, D.; Oettgen, P.; Mercurio, A. M. Transcriptional activation of integrin beta6 during the epithelial-mesenchymal transition defines a novel prognostic indicator of aggressive colon carcinoma. *J. Clin. Invest.* **2005**, *115* (2), 339−347.
(21) Elayadi, A. N.; Samli, K. N.; Prudkin, L.; Liu, Y. H.; Bian, A.; Xie, X. J.; Wistuba, I. I.; Roth, J. A.; McGuire, M. J.; Brown, K. C. A peptide selected by biopanning identifies the integrin alphavbeta6 as a prognostic biomarker for nonsmall cell lung cancer. *Cancer Res.* **2007**, *67* (12), 5889−5895.
(22) Patsenker, E.; Wilkens, L.; Banz, V.; Österreicher, C. H.; Weimann, R.; Eisele, S.; Keogh, A.; Stroka, D.; Zimmermann, A.; Stickel, F. The $\alpha v\beta 6$ integrin is a highly specific immunohistochemical marker for cholangiocarcinoma. *J. Hepatol.* **2010**, *52* (3), 362−369.
(23) Huang, X.; Sheppard, D. Treatment of Acute Lung Injury, Fibrosis and Metastasis with Antagonists of $\alpha v\beta 6$. U.S. Patent 7150871, Dec 19, 2006.
(24) Kogelberg, H.; Tolner, B.; Thomas, G. J.; Di Cara, D.; Minogue, S.; Ramesh, B.; Sodha, S.; Marsh, D.; Lowdell, M. W.; Meyer, T.; Begent, R. H.; Hart, I.; Marshall, J. F.; Chester, K. Engineering a single-chain Fv antibody to alpha v beta 6 integrin using the specificity-determining loop of a foot-and-mouth disease virus. *J. Mol. Biol.* **2008**, *382* (2), 385−401.
(25) Kraft, S.; Diefenbach, B.; Mehta, R.; Jonczyk, A.; Luckenbach, G. A.; Goodman, S. L. Definition of an unexpected ligand recognition motif for alphav beta6 integrin. *J. Biol. Chem.* **1999**, *274* (4), 1979−1985.
(26) Hsiao, J. R.; Chang, Y.; Chen, Y. L.; Hsieh, S. H.; Hsu, K. F.; Wand, C. F.; Tsai, S. T.; Jin, Y. T. Cyclic alphavbeta6-targeting peptide selected from biopanning with clinical potential for head and neck squamous cell carcinoma. *Head Neck* **2010**, *32* (2), 160−172.
(27) Hausner, S. H.; Abbey, C. K.; Bold, R. J.; Gagnon, M. K.; Marik, J.; Marshall, J. F.; Stanecki, C. E.; Sutcliffe, J. L. Targeted in vivo imaging of integrin alphavbeta6 with an improved radiotracer and its relevance in a pancreatic tumor model. *Cancer Res.* **2009**, *69* (14), 5843−5850.
(28) Hausner, S. H.; Kukis, D. L.; Gagnon, M. K.; Stanecki, C. E.; Ferdani, R.; Marshall, J. F.; Anderson, C. J.; Sutcliff, J. L. Evaluation of [^{64}Cu]Cu-DOTA and [^{64}Cu]Cu-CB-TE2A chelates for targeted positron emission tomography with an alphavbeta6-specific peptide. *Mol. Imaging* **2009**, *8* (2), 111−121.
(29) Kimura, R. H.; Teed, R.; Hackel, B. J.; Pysz, M. A.; Chuang, C. Z.; Sathirachinda, A.; Willmann, J. K.; Gambhir, S. S. Pharmacokinetically stabilized cystine knot peptides that bind alpha-v-beta-6 integrin with single-digit nanomolar affinities for detection of pancreatic cancer. *Clin. Cancer Res.* **2012**, *18* (3), 839−849.
(30) Pallaghy, P. K.; Nielsen, K. J.; Craik, D. J.; Norton, R. S. A common structural motif incorporating a cystine knot and a triple-stranded β-sheet in toxic and inhibitory polypeptides. *Protein Sci.* **1994**, *3* (10), 1833−1839.
(31) Colgrave, M. L.; Craik, D. J. Thermal, chemical, and enzymatic stability of the cyclotide kalata B1: the importance of the cyclic cystine knot. *Biochemistry* **2004**, *43* (20), 5965−5975.
(32) Heitz, A.; Avrutina, O.; Le-Nguyen, D.; Diederichsen, U.; Hernandez, J. F.; Gracy, J.; Kolmar, H.; Chiche, L. Knottin cyclization: impact on structure and dynamics. *BMC Struct. Biol.* **2008**, *8*, 54−73.
(33) Werle, M.; Schmitz, T.; Huang, H. L.; Wentzel, A.; Kolmar, H.; Bernkop-Schnurch, A. The potential of cystine-knot microproteins as novel pharmacophoric scaffolds in oral peptide drug delivery. *J. Drug Target* **2006**, *14* (3), 137−146.
(34) Gracy, J.; Le-Nguyen, D.; Gelly, J. C.; Kaas, Q.; Heitz, A.; Chiche, L. KNOTTIN: the knottin or inhibitor cystine knot scaffold in 2007. *Nucl. Acid Res.* **2008**, *36* (Database issue), D314−D319.
(35) Lahti, J. L.; Silverman, A. P.; Cochran, J. R. Interrogating and predicting tolerated sequence diversity in protein folds: application to *E. elaterium* trypsin inhibitor-II cystine-knot miniprotein. *PLoS Comput. Biol.* **2009**, *5* (9), e1000499.
(36) Daly, N. L.; Craik, D. J. Bioactive cystine knot proteins. *Curr. Opin. Chem. Biol.* **2011**, *15* (3), 362−368.
(37) Kimura, R. H.; Cheng, Z.; Gambhir, S. S.; Cochran, J. R. Engineered knottin peptides: a new class of agents for imaging integrin expression in living subjects. *Cancer Res.* **2009**, *69* (6), 2435−2442.
(38) Miao, Z.; Levi, J.; Cheng, Z. Protein Scaffolds Based Molecular Probes for Cancer Molecular Imaging. *Amino Acids* **2011**, *41* (5), 1037−1047.
(39) Hackel, B. J.; Kimura, R. H.; Miao, Z.; Liu, H.; Sathirachinda, A.; Cheng, Z.; Chin, F. T.; Gambhir, S. S. ^{18}F-Fluorobenzoate-labeled cystine knot peptides for PET imaging of integrin $\alpha v\beta 6$. *J. Nucl. Med.* **2013**, *54* (7), 1101−1105.
(40) Levadala, M. K.; Banerjee, S. R.; Maresca, K. P.; Babich, J. W.; Zubieta, J. Direct reductive alkylation of amino acids: synthesis of bifunctional chelates for nuclear imaging. *Synthesis* **2004**, *11*, 1759−1766.
(41) Jiang, L.; Miao, Z.; Kimura, R. H.; Liu, H.; Cochran, J. R.; Culter, C. S.; Bao, A.; Li, P.; Cheng, Z. Preliminary evaluation of ^{177}Lu-labeled knottin peptides for integrin receptor-targeted radionuclide therapy. *Eur. J. Nucl. Med. Mol. Imaging* **2011**, *38* (4), 613−622.
(42) Kimura, R. H.; Levin, A. M.; Cochran, F. V.; Cochran, J. R. Engineered cystine knot peptides that bind $av\beta 3$, $av\beta 5$, and $a5\beta 1$ integrins with low-nanomolar affinity. *Proteins* **2009**, *77* (2), 359−369.
(43) Kimura, R. H.; Jones, D. S.; Jiang, L.; Miao, Z.; Cheng, Z.; Cochran, J. R. Functional mutation of multiple solvent-exposed loops of the Ecballium elaterium trypsin inhibitor-II cystine knot miniprotein. *PLoS One* **2011**, *6* (2), e16112.
(44) Miao, Z.; Ren, G.; Liu, H.; Kimura, R. H.; Jiang, L.; Cochran, J. R.; Gambhir, S. S.; Cheng, Z. An engineered knottin peptide labeled with ^{18}F for PET imaging of integrin expression. *Bioconjugate Chem.* **2009**, *20* (12), 2342−2347.
(45) Liu, S.; Liu, H.; Ren, G.; Kimura, R. H.; Cochran, J. R.; Cheng, Z. PET imaging of integrin positive tumors using 18F labeled knottin peptides. *Theranostics* **2011**, *1*, 403−412.
(46) Nielsen, C. H.; Kimura, R. H.; Withofs, N.; Tran, P. T.; Miao, Z.; Cochran, J.; Cheng, Z.; Felsher, D.; Kjar, A.; Willmann, J. K.;

Gambhir, S. S. PET imaging of tumor neovascularization in a transgenic mouse model using a novel ^{64}Cu-DOTA-knottin peptide. *Cancer Res.* **2010**, *70* (22), 9022−9030.
(47) Jiang, L.; Miao, Z.; Kimura, R. H.; Silverman, A. P.; Ren, G.; Liu, H.; Lu, H.; Cochran, J. R.; Cheng, Z. ^{111}In-labeled cystine-knot peptides based on the Agouti-related protein for targeting tumor angiogenesis. *J. Biomed. Biotechnol.* **2012**, *2012*, 368075.
(48) Jiang, L.; Kimura, R. H.; Miao, Z.; Silverman, A. P.; Ren, G.; Liu, H. G.; Li, P.; Gambhir, S. S.; Cochran, J. R.; Cheng, Z. Evaluation of a ^{64}Cu-labeled cystine-knot peptide based on Agouti-Related protein for PET of tumors expressing $\alpha_v\beta_3$ integrin. *J. Nucl. Med.* **2010**, *51* (2), 251−258.
(49) Jiang, H.; Moore, S. J.; Liu, S.; Liu, H.; Miao, Z.; Cochran, F. V.; Liu, Y.; Tian, M.; Cochran, J. R.; Zhang, H.; Cheng, Z. A novel radiofluorinated agouti-related protein for tumor angiogenesis imaging. *Amino Acids* **2013**, *44* (2), 673−681.
(50) Kimura, R. H.; Miao, Z.; Cheng, Z.; Gambhir, S. S.; Cochran, J. R. A dual-labeled knottin peptide for PET and near-infrared fluorescence imaging of integrin expression in living subjects. *Bioconjugate Chem.* **2010**, *21* (3), 436−444.
(51) Bartholomä, M.; Valliant, J.; Maresca, K. P.; Babich, J.; Zubieta, J. Single amino acid chelates (SAAC): a strategy for the design of technetium and rhenium radiopharmaceuticals. *Chem. Commun.* **2009**, *5*, 493−512.
(52) Maresca, K. P.; Hillier, S. M.; Femia, F. J.; Zimmerman, C. N.; Levadala, M. K.; Banerjee, S. R.; Hicks, J.; Sundararajan, C.; Valliant, J.; Zubieta, J.; Eckelman, W. C.; Joyal, J. L.; Babich, J. W. Comprehensive radiolabeling, stability, and tissue distribution studies of technetium-99m single amino acid chelates (SAAC). *Bioconjugate Chem.* **2009**, *20* (8), 1625−1633.
(53) Maresca, K. P.; Marquis, J. C.; Hillier, S. M.; Lu, G.; Femia, F. J.; Zimmerman, C. N.; Eckelman, W. C.; Joyal, J. L.; Babich, J. W. Novel polar single amino acid chelates for technetium-99m tricarbonyl-based radiopharmaceuticals with enhanced renal clearance: application to octreotide. *Bioconjugate Chem.* **2010**, *21* (6), 1032−1042.
(54) Jiang, H.; Kasten, B. B.; Liu, H.; Qi, S.; Liu, Y.; Tian, M.; Barnes, C. L.; Zhang, H.; Cheng, Z.; Benny, P. D. $M(CO)_3$ (M = Re, ^{99m}Tc) incorporation on the backbone of an α-MSH peptide using a modified-cysteine chelation strategy. *Bioconjugate Chem.* **2012**, *23* (11), 2300−2312.